Analysis and Simulation of the Grid-tied Inverter and its Control in the Synchronous Reference Frame

*[1]Olarinoye, G. A. and [2]Omeiza, I. O. A.

[1]Department of Electrical Engineering, Ahmadu Bello University Zaria, Nigeria.
[2]Department of Electrical and Electronics Engineering, University of Ilorin, Ilorin, Nigeria.

Article Information	Abstract
	The grid-tied inverter is one way to interface renewable power sources such as solar PV, batteries, fuel cells and wind power to the utility grid and ensure efficient conversion, control and exchange of electric power from these sources to the utility grid and vice-versa. The grid-tied inverter also alleviates the challenges of satisfying grid code standards which power system operators demand for renewable energy integration to the grid. In this paper, the model of the grid-tied inverter and associated controllers is developed, analyzed and simulated for active and reactive power flow control. A reference current with a magnitude of 114A is demonstrated to provide active and reactive power flow of 100kW and 100kVA respectively to a three-phase power grid via current control using two PI controllers in the synchronous reference frame. The three-phase inverter is powered from a dc voltage of 800V. Simulation results of active power, reactive power, inverter and grid voltages and currents prove the effectiveness of the PLL and current control method applied for a stable and reliable power supply from the dc source to the grid.

***Corresponding Author: Olarinoye, G.A.;** baolarinoye@abu.edu.ng

Introduction

In recent times, the Nigerian government has taken the initiative to promote renewable power generation sources such as hydro and solar plants. This is part of efforts to meet the ever-increasing demand for electrical energy in the country. It is also an effort to mitigate greenhouse gas emissions, global warming and climate change phenomena associated with the production of electrical energy from fossil fuels (Energy Commission of Nigeria, 2005; Vendoti *et al.*, 2024; Masum and Mamun, 2024). It is estimated that by 2025 the share of renewable energy generation will account for 10% of Nigeria's total energy consumption (Nigeria Renewable Energy Master Plan, 2014). This plan coupled with the recent revelation by the Federal Government of Nigeria to increase power generation from a paltry 4000 to 6000MW by the end of 2024, through the deployment of hydro and solar power plants will very likely see the emergence of grid-tied inverter solutions in the national grid. Renewable energy sources are intermittent and cannot be connected directly to the utility grid (Patel, Gupta and Babu, 2019; Qureshi and Potdar, 2021; Vendoti *et al*., 2024). Besides, dc power from sources such as solar panels need to be converted to ac power before it can be injected into the utility grid (Blaabjerg *et al.*, 2006; Fatima, Siddiqui and Sinha, 2024). Moreover, power system operators require that certain standards be met to ensure adequate connection of renewable energy sources such as photovoltaic panels and wind energy conversion systems to the utility grid (Blaabjerg, 2006; Evju, 2007). These standards include high power conversion efficiency, control of active and reactive power, low Total Harmonic Distortion (THD) of grid current, grid synchronization, excellent transient response and maximum power extraction among other requirements (Patel, Gupta and Babu, 2019). One way to achieve these standards is through the use of the grid-tied inverter and its control strategy (Blaabjerg *et al.*, 2006; Marangalu *et al.*, 2024; Kumar *et al.*, 2024). The inverter converts variable or constant DC power to a controllable AC power at high efficiency and its control strategy is a key consideration to meeting the grid code requirements of power system operators and therefore ensuring proper integration between the renewable energy source and the grid (Masum and Mamun, 2024; Fatima, Siddiqui and Sinha, 2024). Some of the grid codes include IEEE 1547, IEEE 929, IEC 61727 and IEC61400. They are established by the Institute of Electrical and Electronics Engineers (IEEE) and the International Electrotechnical Commission (IEC) (Evju, 2007; MacDowell *et al.*, 2019). The grid-tied inverter is designed to transfer controllable power (active or reactive) at the given voltage and to facilitate synchronization between its output and the

utility grid (Kumar *et al*., 2024). The grid-tied inverter structure is illustrated in Figure 1.
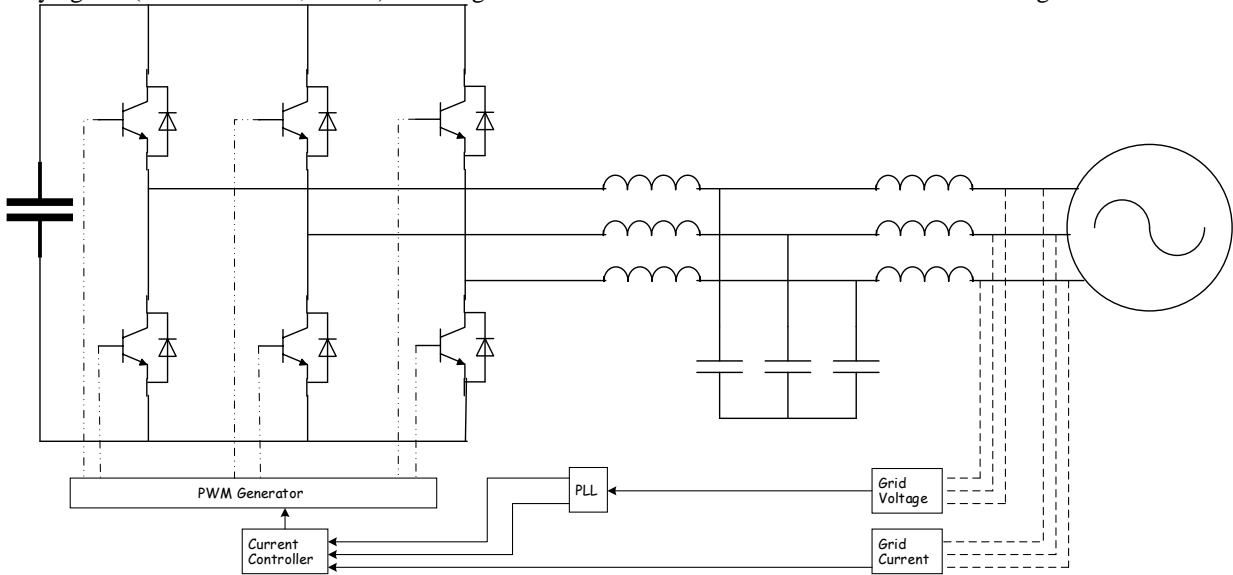

Figure 1: Grid-tied Inverter

The grid-tied inverter finds applications in the active front end in which the inverter on the grid side is connected to another inverter that is used to control an ac motor. Such application is shown in Figure 2 (Teodorescu, Liserre and Rodriguez, 2011).
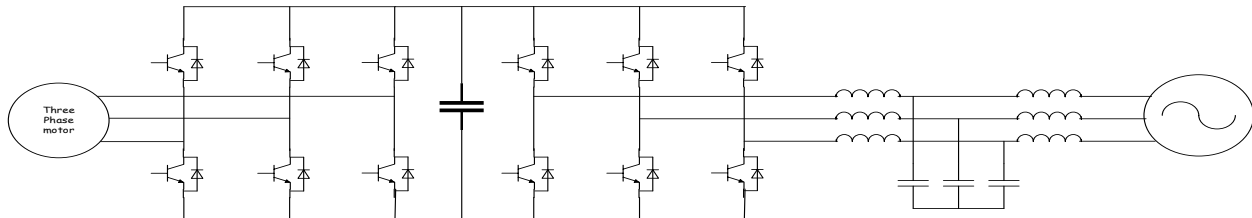

Figure 2: Active front-end

The active front end allows for bi-directional power flow. The associated control makes it possible for the system to operate in the four-quadrant mode and the grid current is controlled to give an undistorted sinusoidal waveform with low harmonic content. Other applications include vehicle-to-grid (V2G) technologies (Sadabadi *et al.*, 2023) and energy management. Figure 3 presents the structure of the grid-tied inverter as applied in energy management (Teodorescu, Liserre and Rodriguez, 2011; Vendoti *et al.*, 2024). In this configuration, the Grid-tied inverter is connected to a DC-DC converter through a filter. The DC-DC converter is then connected to a combination of solar panels, batteries and/or fuel cells. The energy management system and associated control may then decide the direction of power flow in the system.
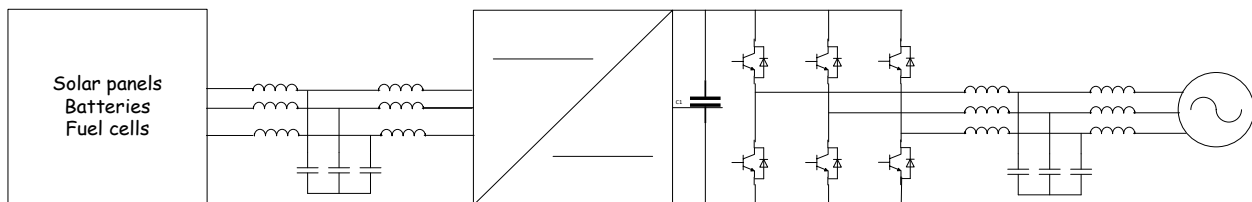

Figure 3: Energy management system

Grid-connected inverters are operated in the direct power, voltage, PQ or current control mode for transfer of power to the utility grid (Shah, 2015; Kumar *et al*., 2024). The control can become complex depending on whether the control mode is grid-supporting or grid-forming. A study of a three-phase two-stage solar PV Inverter for grid connection was conducted in Fatima, Siddiqui and Sinha (2022). The system was implemented in MATLAB/Simulink. Although active power flow to the grid was demonstrated, the analysis of the grid-tied inverter and its control algorithm was not evident in the work, which makes it difficult for a reader to understand the system model and the interaction between the inverter and the grid. A grid-connected inverter with a neutral wire was developed in Patel, Gupta and Babu (2019) to work as a multifunctional inverter. It was controlled to inject active power into the grid as well as to generate harmonic compensating current in a grid-supporting mode. A hysteresis controller was used for current control in the stationary reference frame but the control is quite complex.

The objective of this paper is to develop and analyze the model of the three-phase grid-tied inverter and its associated current controllers. The model is then simulated in MATLAB/Simulink software the results obtained are carefully presented and discussed. A simple control strategy is demonstrated in which the real and reactive components of the grid current are controlled for real and reactive power flow to the grid. The grid voltages and currents are transformed to a reference frame rotating at the same frequency as the grid voltages. This reference frame is also known as the synchronous reference frame and it makes it easy to achieve control through linear PI controllers. The paper is organized as follows; section 2 provides the development of the models of the three-phase inverter, grid-tied inverter, inverter control, controller design and the phase-locked loop for grid synchronization.   Section three presents the simulation results and discussion while section 4 concludes   the   paper.

Three-phase Inverter Model
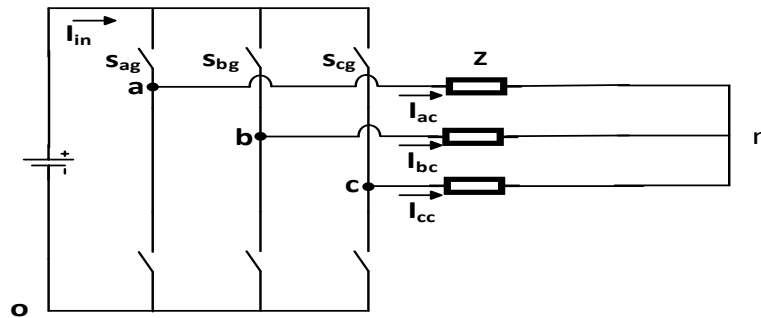The three-phase inverter topology is shown in Figure 4.

Figure 4: Three-phase inverter

The output voltages referred to the negative point of the DC bus v_{ao}, v_{bo} and v_{co} can be obtained from the Figure as follows;

$$v_{ao} = V_{dc}s_{ag} \qquad (1)$$

Inverter output voltages are synthesized by commanding the appropriate switching pulses of the

By   different combinations of these pulses, it is possible to create AC output voltages with fundamental components of different amplitude and frequency. Phase voltages v_{an}, v_{bn} and v_{cn} are derived from Figure 4 as follows;

$$v_{bo} = V_{dc}s_{bg} \qquad (2)$$
$$v_{co} = V_{dc}s_{cg} \qquad (3)$$
where s_{ig} $\in \{0,1\}$ and $i = a, b, c$.

Insulated Gate Bipolar Transistors (IGBTs) of the inverter i.e. s_{ag}, s_{ag} and s_{ag}.

$$v_{an} = v_{ao} - V_{no} \qquad (4)$$
$$v_{bn} = v_{bo} - V_{no} \qquad (5)$$
$$v_{cn} = v_{co} - V_{no} \qquad (6)$$

where V_{no} is the voltage between the negative rail of Phase voltages with respect to the switching functions/commands are derived from (1) – (6) and provided as follows;

$$v_{an} = \frac{V_{dc}}{3}\left(2s_{ag} - s_{bg} - s_{cg}\right) \qquad (7)$$
$$v_{bn} = \frac{V_{dc}}{3}\left(2s_{bg} - s_{ag} - s_{cg}\right) \qquad (8)$$
$$v_{cn} = \frac{V_{dc}}{3}\left(2s_{cg} - s_{ag} - s_{bg}\right) \qquad (9)$$

Three phase Line voltages are obtained from phase voltages using the following relationships;

$$v_{ab} = v_{an} - v_{bn} \qquad (10)$$
$$v_{bc} = v_{bn} - v_{cn} \qquad (11)$$
$$v_{ca} = v_{cn} - v_{an} \qquad (12)$$

The three-phase inverter is controlled using the technique of sine pulse width modulation (SPWM)

the inverter and the neutral point of the load. among many other options which include the third harmonic injection, space vector modulation, etc. A triangular carrier signal, V_{tri} is compared with the reference or modulating signal and for a Unipolar SPWM, the inverter output voltages are created with commands s_{ag}, s_{bg} and s_{cg} taking values of logic '1' whenever the modulating signals v_{ab}^*, v_{bc}^*, $v_{ca}^* > V_{tri}$. v_{ab}^*, v_{bc}^*, v_{ca}^* are also referred to as the reference voltages for lines a, b and c respectively. These reference or modulating signals are the direct result of the current control algorithm. When compared with the triangular signal, switching functions or pulses are generated for the control of the inverter switches.

Grid-tied Inverter Model

The d-q model equations of the grid inverter with LCL filter is now developed from the space vector model of the grid-tied inverter. The equivalent circuit is provided in Figure 5.
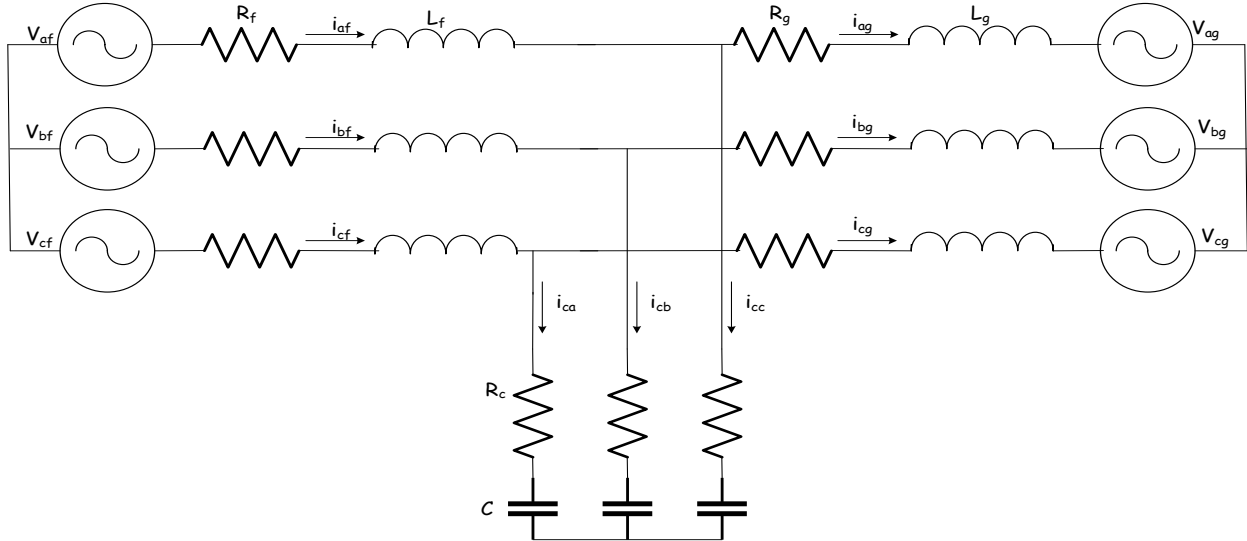

Figure 5: Equivalent circuit of the grid-tied inverter

Using linear circuit theory, the equations describing the grid-tied inverter system of Figure 5 is derived as;

$$v_{af} = R_f i_{af} + L_f p i_{af} + v_{ca} \qquad (13)$$
$$v_{bf} = R_f i_{bf} + L_f p i_{bf} + v_{cb} \qquad (14)$$
$$v_{cf} = R_f i_{cf} + L_f p i_{cf} + v_{cc} \qquad (15)$$
$$v_{ca} = R_g i_{ag} + L_g p i_{ag} + v_{ag} \qquad (16)$$
$$v_{cb} = R_g i_{bg} + L_g p i_{bg} + v_{bg} \qquad (17)$$
$$v_{cc} = R_g i_{cg} + L_g p i_{cg} + v_{cg} \qquad (18)$$

L_f is the inductance of the inverter side of the filter. R_f is the parasitic resistance of the inverter-side filter. L_g and R_g are the inductance and parasitic resistance

of the grid side of the filter respectively. v_{af}, v_{bf} and v_{cf} are the phase voltages of the inverter. i_{af}, i_{bf} and i_{cf} are the output currents of the inverter. v_{ag}, v_{bg} and v_{cg} are the grid voltages while i_{ag}, i_{bg} and i_{cg} are the grid currents. The voltage across the capacitor branch is described by the following equations;

$$v_{ca} = R_c i_{ca} + \frac{1}{C}\int i_{ca}\,dt \qquad (19)$$
$$v_{cb} = R_c i_{cb} + \frac{1}{C}\int i_{cb}\,dt \qquad (20)$$
$$v_{cc} = R_c i_{cc} + \frac{1}{C}\int i_{cc}\,dt \qquad (21)$$

R_c and C are the damping resistance and capacitance of the filter. The space vector model of equations (13)-(18) in the synchronous reference frame is given as follows (Abad, 2017);

$$\boldsymbol{v}_f^e = R_f \boldsymbol{i}_f^e + L_f p\boldsymbol{i}_f^e + R_g \boldsymbol{i}_g^e + L_g p\boldsymbol{i}_g^e + \boldsymbol{v}_g^e + j\omega_e L_f \boldsymbol{i}_f^e + j\omega_e L_g \boldsymbol{i}_g^e \quad (22)$$

Equations (22)-(26) can be used to obtain the d-q model of the grid-tied inverter and is given as;

$$v_{df} = R_f i_{df} + L_f p i_{df} + R_g i_{dg} + L_g p i_{dg} + v_{dg} - \omega_e L_f i_{qf} - \omega_e L_g i_{qg} \quad (27)$$

$$v_{qf} = R_f i_{qf} + L_f p i_{qf} + R_g i_{qg} + L_g p i_{qg} + v_{qg} + \omega_e L_f i_{df} + \omega_e L_g i_{dg} \quad (28)$$

Equations (29) and (30) are first-order non-linear systems for which v_{df} and v_{qf} are inputs and i_d and i_q are outputs. The voltage commands needed to give the desired currents, i_d and i_q, are obtained with a feedback-based solution using current controllers. The formulation for the controller gains will be performed using equations (29) and (30). Expressions $\omega_e(L_f + L_g)i_q$ and $\omega_e(L_f + L_g)i_d$ in the equations are cross-coupling terms (Gupta *et al*., 2022; Abad,

where ω_e is the angular frequency of the grid voltage. $\boldsymbol{v}_f^e$, $\boldsymbol{v}_g^e$ $\boldsymbol{i}_g^e$ and $\boldsymbol{i}_f^e$ are space vectors in the synchronous reference frame and are defined as;

$$\boldsymbol{v}_f^e = v_{df} + jv_{qf} \quad (23)$$
$$\boldsymbol{v}_g^e = v_{dg} + jv_{qg} \quad (24)$$
$$\boldsymbol{i}_f^e = i_{df} + ji_{qf} \quad (25)$$
$$\boldsymbol{i}_g^e = i_{dg} + ji_{qg} \quad (26)$$

If we assume that $i_{df} \approx i_{dg} = i_d$ and $i_{qf} \approx i_{qg} = i_q$ then equations (27)-(28) become

$$v_{df} = (R_f + R_g)i_d + (L_f + L_g)p i_d + v_{dg} - \omega_e(L_f + L_g)i_q \quad (29)$$

$$v_{qf} = (R_f + R_g)i_q + (L_f + L_g)p i_q + v_{qg} + \omega_e(L_f + L_g)i_d \quad (30)$$

2017) which will be cancelled in the control structure to provide for a linear control of current. Three phase active and reactive power are expressed in d-q reference frame as follows; (Abad, 2017)

$$P = \frac{3}{2}(v_q i_q + v_d i_d) \quad (31)$$
$$Q = \frac{3}{2}(v_q i_d - v_d i_q) \quad (32)$$

Where P and Q are the active and reactive power respectively. Either of the quantities can be controlled by controlling the d-q currents.

Inverter Control

The block diagram of the current control strategy is provided in Figure 6. It is based on the synchronous reference frame theory.
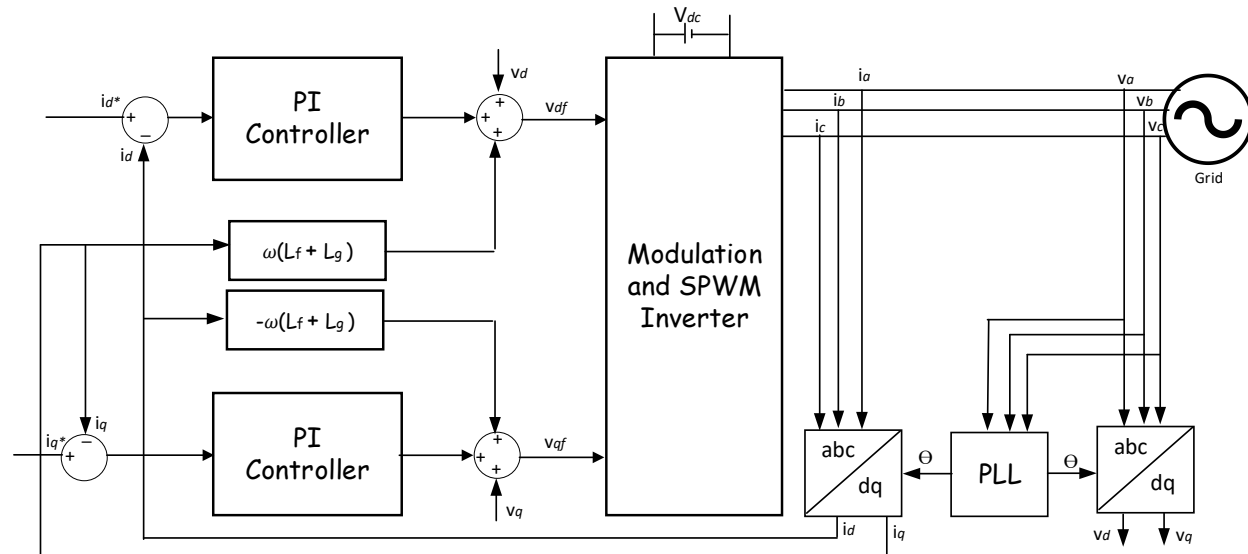

Figure 6: Current control in the synchronous reference frame

As seen in Figure 6, the grid voltages are sensed and transformed first to their equivalent synchronous reference frame or d-q voltages where they become DC quantities and are then used for inverter control

(Abad, 2017; Blaabjerg, 2006; Evju, 2007). Inverter three-phase currents are sensed and transformed as well to their d-q equivalents. Control is performed in the synchronous reference frame in which the active

component of the inverter current i_d is regulated to provide active power control. The reactive component of the inverter current i_q is regulated as well to provide reactive power control. PI controllers are employed for the current control. Despite their drawbacks of poor compensation capability of low order harmonics, PI controllers still give a very

Controller Design
From equations (29) and (30), after the cancellation of the coupling terms, the model equations at open loop for the LCL filter yield the following;

$$V_{df} = (R_f + R_g)i_d + (L_f + L_g)pi_d \qquad (33)$$
$$V_{qf} = (R_f + R_g)i_q + (L_f + L_g)pi_q \qquad (34)$$

The cancellation of the cross-coupling terms is carried out at the output of the PI controllers.

satisfactory response when controlling DC variables. The reference currents i_d^* and i_q^* and the actual currents are used to generate error signals which are passed to their corresponding PI controllers as seen in Figure 6.

For this system of equations, applying the Laplace transformation produces the following transfer functions;

$$\frac{i_d(s)}{V_{df}(s)} = \frac{1}{[(L_f+L_g)s+(R_f+R_g)]} \qquad (35)$$

$$\frac{i_q(s)}{V_{qf}(s)} = \frac{1}{[(L_f+L_g)s+(R_f+R_g)]} \qquad (36)$$

v_{dg} and v_{qg} are added to the output of the PI controllers as feed-forward terms as can be observed in Figure 7.
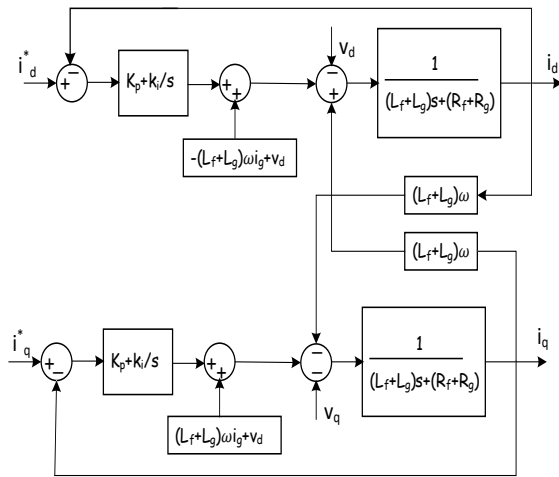

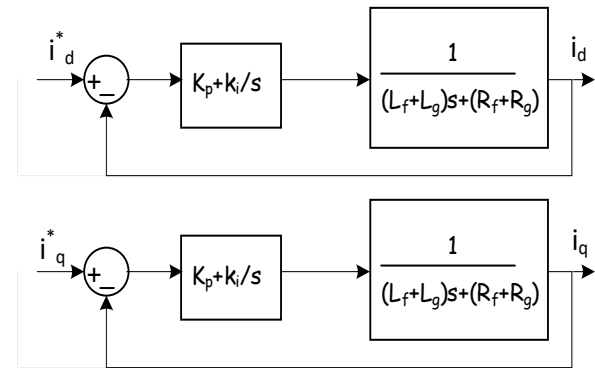Figure 7: Current control structure for the LCL filter

The ideal PI control loop is provided in the block diagram of Figure 8.

Issues such as the effects of switching delays and other non-linearities and presence of harmonics have been neglected for simplicity. The current closed loops can be represented ideally according to the following transfer functions;

$$\frac{i_d(s)}{i_d^*(s)} = \frac{sk_p+k_i}{[(L_f+L_g)s^2+s(R_f+R_g+k_p)+k_i]} \qquad (37)$$

$$s^2 + s\left(\frac{R_f+R_g+k_p}{L_f+L_g}\right) + \frac{k_i}{L_f+L_g} \equiv s^2 + 2\zeta\omega_n s + \omega_n^2 =$$
$$(s + \omega_n)^2 \qquad (39)$$

Figure 8: Ideal Current Control loop

$$\frac{i_q(s)}{i_q^*(s)} = \frac{sk_p+k_i}{[(L_f+L_g)s^2+s(R_f+R_g+k_p)+k_i]} \qquad (38)$$

The expressions for the PI controller gains, k_p and k_i were obtained by comparing the normalized denominator of equation (37) with the standard second order denominator, as follows;

where upon k_p and k_i were obtained as;

$$k_p = (L_f + L_g)2\zeta\omega_n - (R_f + R_g) \qquad (40)$$
$$k_i = (L_f + L_g)\omega_n^2 \qquad (41)$$

The PI controller gains are calculated as 0.24 and 157 for k_p and k_i respectively using the parameters of

v_{df} and v_{qf} are therefore multiplied by $\frac{2}{V_{dc}}$ to obtain m_d and m_q which are transformed to the *abc* reference frame to produce the voltage references for

Phase Locked Loop
For the three-phase voltage and current transformations, the phase angle θ of the grid voltage is needed. This angle is estimated by the phase-locked loop (PLL). The PLL block is presented in Figure 9. Its closed-loop nature provides stability and perturbation rejections to the angle estimation. It is a
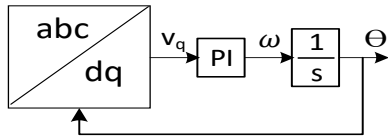

Figure 9: Phase locked loop

assuming double real poles. ζ is the damping ratio. ω_n is the natural frequency.

Table 1. For the SPWM, the relationship between modulation index and inverter voltages are given as;
$$v_{df} = m_d \frac{V_{dc}}{2} \qquad (42)$$
$$v_{qf} = m_q \frac{V_{dc}}{2} \qquad (43)$$

the three-phase inverter control. It is these references that are applied to the SPWM block to generate the commands for the inverter switches.

simple but effective synchronization method. It synchronizes the inverter frequency to the grid voltage frequency. The PLL is synchronized by using the *d-q* coordinates of the grid voltages as seen in Figure 9. It extracts the phase angle from the grid voltages to keep the controlled current in phase with the grid voltage.

Table 1: Table of Parameters

PARAMETERS	VALUES
RATED POWER	10kVA
V_{grid}	415V
V_{dc}	800V
f_{sw}	10kHz
R_f	0.01Ω
R_g	0.01Ω
L_f	0.5mH
L_g	0.5mH
C	100μF
ζ	1
ω_n	20 rad/s

Simulation Results and Discussion
The inverter output voltage is shown in Figure 10 and the grid voltages are shown in Figure 11(a). Whereas the inverter output voltages are square waveforms containing harmonics of the switching frequency, the grid voltages are sinusoidal waveforms. The LCL filter is very effective in filtering out the high-frequency harmonics of the inverter voltage. The grid currents are shown in Figure 11(b). They can be observed to be sinusoidal three-phase currents that are 120^0 out of phase with one another. Active power flow control is performed by setting the reactive component of the current i_q equal to zero and setting

a non-zero reference for the active current component of power. With the active current component set to -114A (which corresponds to a rated power of 100kW) initially, only active power flows to the grid. There is no reactive power flow. This is demonstrated in the result of Figure 11(c) by the fact that the grid current is in phase with the grid voltage, indicating that the power factor is unity. The reference current was reduced, by half, to -56A at a time of 0.5s of simulation time while still maintaining the reactive component at a value of zero. This is the reason why the grid current is seen to reduce by half in Figures 11(b) and (c).
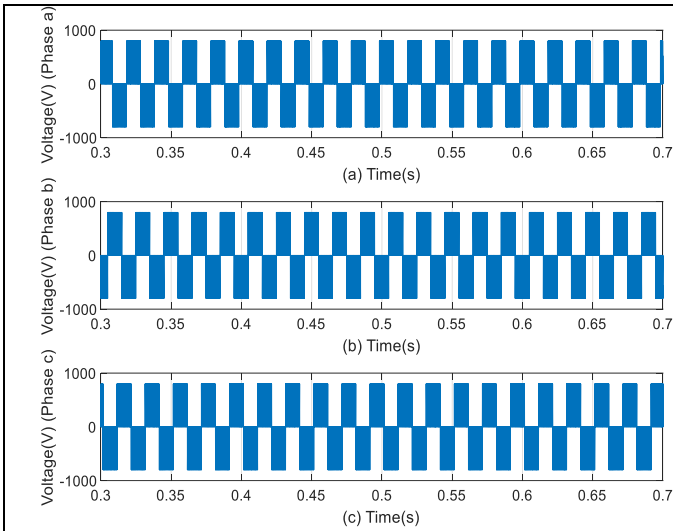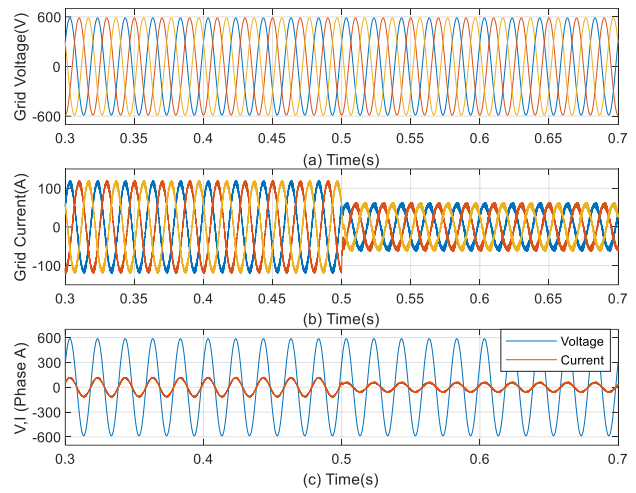
Figure 10: Inverter output voltages

Figure 11: (a) Grid voltages (b) Grid currents (c) Voltage and current of Phase '*a*'

The plot of active and reactive power can be seen in Figure 12. Clearly, Reactive power under this condition is zero. The active power is observed to be equal to 100kW initially and then this value is reduced by half from the time of 0.5s following the reference value set for the active current component. To send reactive power to the grid, a reference of

114 A was also set for the reactive component of current and a reference value of zero was set for the active component of current (i.e. i_d). Figure 13 shows the results under this condition. It can be seen that the active power is now equal to zero while the reactive power is equal to 100kVA.
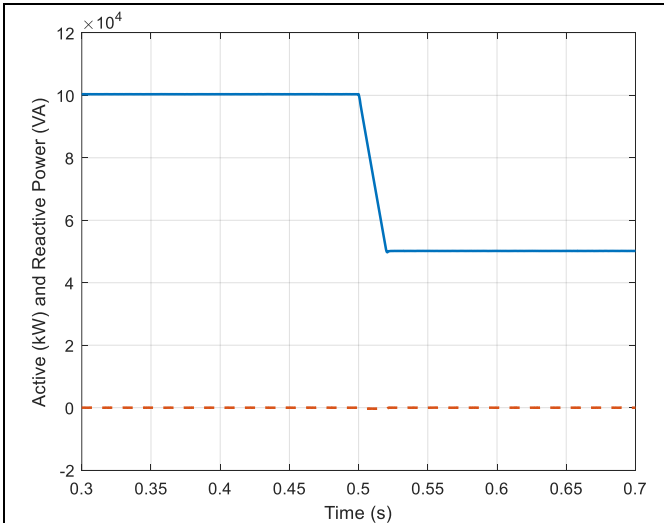

Figure 12: Active and reactive power under active power flow conditions
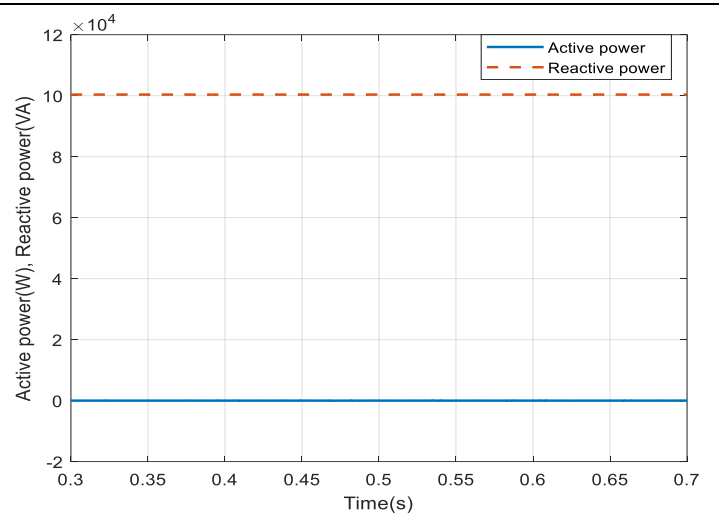

Figure 13: Active and reactive power under reactive power flow conditions

The grid voltage and current are now seen to be out of phase with each other in Figure 14, indicating reactive power flow. The peak value of the current can be seen to be equal to the reference value of the

reactive component of the current. It is clear that simulation results verify the analysis outlined in section 2.
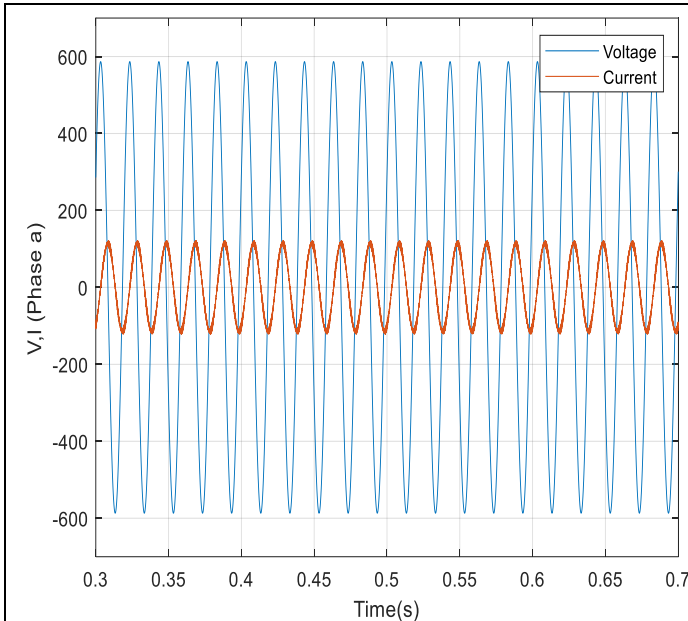
Figure 14: Voltage and current of phase 'a' under reactive power flow conditions
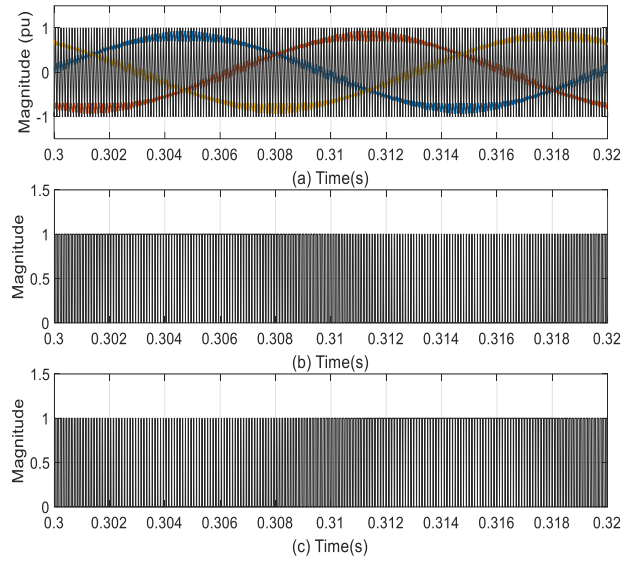

Figure 15: (a) modulating and carrier signals (b) switching pulse for top switch of phase 'a' (c) switching pulse for bottom switch of phase 'a'

The modulating signals passed to the PWM generator and the triangular carrier signal of 10kHz are presented in Figure 15(a). It can be seen that the process is not over modulated or under modulated. Modulation signals have a magnitude slightly less than 1 which is appropriate. The switching pulses for the top and bottom switches of phase 'a' of the Inverter, are shown in Figures 15(a) and (b). The phase angle of the grid voltage, θ, is illustrated in Figure 16a. It is the output of the PLL and it can be seen that it changes from 0 to 314 radians between 0 and 1s giving a constant angular frequency of 314 rad/s for the grid voltage and current as seen in Figure 16(b).
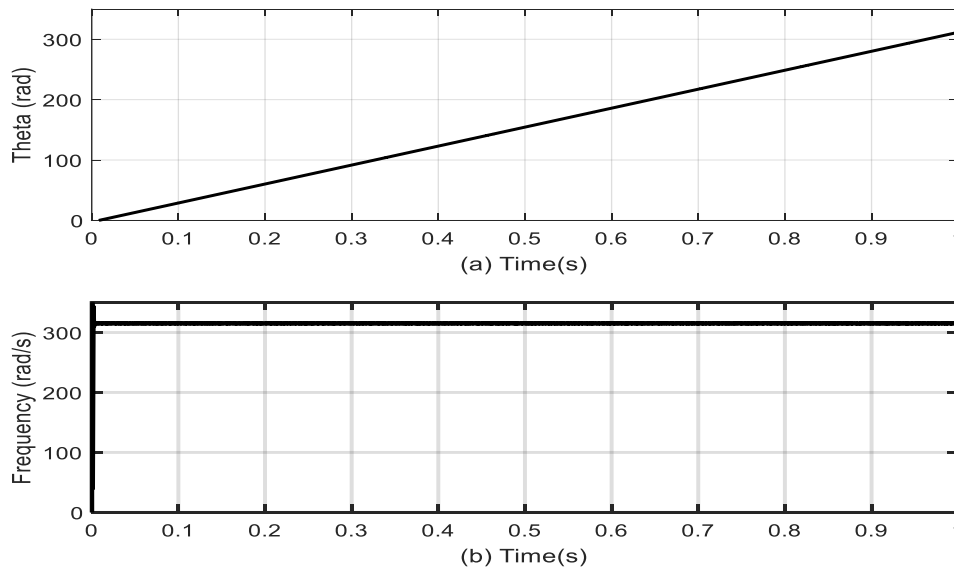

Figure 16: (a) Phase angle of grid voltage and current (b) frequency of grid voltage and current

Conclusion

The operation of the grid-tied inverter in the synchronous reference frame has been demonstrated in this paper. The model of the three-phase inverter, grid-tied inverter and control structure were developed, analyzed and simulated in the MATLAB/Simulink environment. Active and reactive power flow control in the synchronous reference frame was effectively demonstrated. A reference value of -114 A was set for the active component of current while a value of zero was set for the reactive component of current thereby producing active power of 100kW at the three-phase power grid. Grid voltages and currents were observed to be in phase under this condition. A similar procedure was performed for the reactive power control as well. Reactive power control is necessary because of grid voltage stability and grid interactions with non-linear loads such as power converters, transformers and induction motors. A *dq* current controller with PI control was developed and designed and a simple PLL was adopted to realize the control in the synchronous reference frame. Simulation results of active power, reactive power, inverter and grid voltages and currents prove the effectiveness of the PLL and current control method applied in this work. Although this control approach is fairly easy to understand, the cancellation terms and the voltage feed-forward approach discourages implementation. Besides, low order harmonic compensation which is usually required for overcoming power quality issues during the occurrence of disturbances is impractical with linear PI controllers. Other controllers such as proportional resonance (PR), hysteresis and dead-beat current controllers are often preferred to the PI current controllers and are recommended because of their fast dynamics and ease of implementation.

References

Abad, G. (2017). Power electronics and electric drives for traction applications. John Wiley and Sons. United Kingdom.

Blaabjerg, F., Teodorescu, R., Liserre, M. and Timbus, A. V. (2006). Overview of Control and Grid Synchronization for Distributed Power Generation Systems. *IEEE Transactions on Industrial Electronics*. 53(5): 1398-1409. doi: 10.1109/TIE.2006.881997.

Energy Commission of Nigeria (2005). Renewable energy master plan, Final report. Section 1.5 – 1.7 - Nigeria's renewable energy vision, p35 – 38. Retrievedfromhttps://www.iceednigeria.org/resources/nov.-2005.pdf

Fatima, M., Siddiqui, A. S. and Sinha, S. K. (2024). Utilizing Feedforward Compensation, Active and Reactive Power Control of a Grid-Tied Three-Phase Inverter. *IEEE International Conference on Computing, Power and Communication Technologies (IC2PCT)*, Greater Noida, India, pp. 802-806, doi: 10.1109/IC2PCT60090.2024.10486684.

Fatima, M., Siddiqui, A. S. and Sinha, S. K. (2022). Implementation of Three-Phase two Stage Solar PV Inverter for Grid Connection. *8th International Conference on Advanced Computing and Communication Systems (ICACCS),* Coimbatore, India, pp. 1325-1329, doi: 10.1109/ICACCS54159.2022.9785351.

Gupta, A. K., Pragallapati, N., Joshi, M. S. and Agarwal, V. (2022). A Novel Per Unit (P.U.) Integer Format Applied to the Control of a Grid-Tied Solar PV Inverter. *IEEE Transactions on Industrial Informatics.* 18(2): 735-743. doi: 10.1109/TII.2021.3067922

Kumar, R., Chaudhari M. A. and Chaturvedi, P. (2024). Analysis of Synchronverter and PLL-Less Control for Three-Phase VSI in AC Microgrids. *Third International Conference on Power, Control and Computing Technologies (ICPC2T),* Raipur, India, pp. 810-816, doi 10.1109/ICPC2T60072.2024.10474759.

MacDowell, J., Wang, Y., Quint, R., Chi, Y., Ernst, B., Saylors, S., Jacobson, D., Andresen, B., Sørensen, P. E., Portales, R., Brake, D., Zavadil, B. and Robinson, L. (2019). A Journey Through Energy Systems Integration: Trending Grid Codes, Standards and IEC Collaboration. *IEEE Power and Energy Magazine*. 17(6): 79-88. doi: 10.1109/MPE.2019.2933282.

Marangalu, M. G., Kurdkandi, N. V., Monfared, K. K., Talebian, I., Neyshabouri, Y. and Vahedi, H. (2024). A New High Step-Up SC-Based Grid-Tied Inverter with Limited Charging Spike for RES Applications. *IEEE Open Journal of Power Electronics.* 5: 295-310. doi: 10.1109/OJPEL.2024.3366165.

Masum, S. M. and Al Mamun E. (2024). Comparative Study of Grid-Tied PV Systems in Bangladesh's Coastal Gems. *International Conference on Green Energy, Computing and Sustainable Technology (GECOST),* Miri Sarawak, Malaysia, pp. 420-424, doi: 10.1109/GECOST60902.2024.10474676.

Nigeria Renewable Energy Master Plan (2014). International Energy Agency. Retrieved 2nd August 2014.

Patel, N., Gupta, N. and Babu, B. C. (2019). Design, Development and Implementation of Grid-Connected Solar Photovoltaic Power Conversion System. *Energy Sources, Part A: Recovery, Utilization and Environmental Effects.* 43(22): 2915-2934. https://doi.org/10.1080/15567036.2019.1668506

Qureshi, S. A and Potdar, M. S. (2021). A Comparative Analysis & Simulation of Phase Locked Loop for a Grid synchronized Photovoltaic System. *IEEE International Conference on Mobile Networks and Wireless Communications (ICMNWC)*, Tumkur, Karnataka, India, pp. 1-7, doi: 10.1109/ICMNWC52512.2021.9688442.

Sadabadi, M. S., Sharifzadeh, M., Mehrasa, M., Karimi, H. and Al-Haddad, K. (2023). Decoupled *dq* Current Control of Grid-Tied Packed E-Cell Inverters in Vehicle-to-Grid Technologies. *IEEE Transactions on Industrial Electronics.* 70(2): 1356-1366. doi: 10.1109/TIE.2022.3156160.

Shah, S. (2015). Step-by-step Design of an LCL Filter for Three-phase Grid Interactive Converter. Retrieved from
 http://dx.doi.org/10.13140/RG.2.1.3883.696410.

Evju, S. E. (2007). Fundamentals of Grid Connected Photo-Voltaic Power Electronic Converter Design. Unpublished MSc thesis in Energy and Environment. Department of Electrical Power Engineering, Norwegian University of Science and Technology

Teodorescu R., Liserre M., Rodriguez P. (2011). Grid converters for photovoltaic and wind power systems. John Wiley and Sons. USA.

Vendoti, S., Inayathullaah, M. A., Chiranjivi, M., Fabbina, C., Kavin, K. S. and Malathi, P. (2024). A WECS fed Grid Tied DC-DC LUO Converter for Energy Management in Electric Vehicle System. *2nd International Conference on Computer, Communication and Control (IC4)*, Indore, India, pp. 1-7, doi: 10.1109/IC457434.2024.10486647.